AGU PUBLICATIONS

Water Resources Research

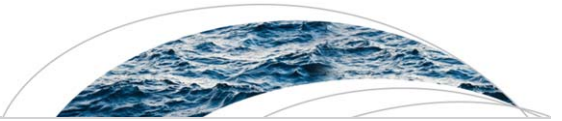

RESEARCH ARTICLE
10.1002/2016WR020062

What Determines Water Temperature Dynamics in the San Francisco Bay-Delta System?

J. Vroom[1], M. van der Wegen[1,2], R. C. Martyr-Koller[3], and L. V. Lucas[4]

[1]Deltares, Unit Marine and Coastal Systems, Delft, The Netherlands, [2]Water Science and Engineering Department, UNESCO-IHE, Delft, The Netherlands, [3]Department of Civil and Environmental Engineering, University of California Berkeley, Berkeley, CA, USA, [4]United States Geological Survey, Menlo Park, CA, USA

Key Points:
- Our modeling approach shows significant skill in predicting daily, seasonal, and yearly observed temperatures in San Francisco Estuary
- Thermal stratification occurs limitedly at Delta monitoring stations while considerable vertical thermal gradients prevail in North Bay
- Atmospheric forcing, amount, and temperature of inflows influence Delta temperatures, while ocean temperature has a negligible effect

Supporting Information:
- Supporting Information S1

Correspondence to:
J. Vroom,
julia.vroom@deltares.nl

Citation:
Vroom, J., van der Wegen, M., Martyr-Koller, R. C., & Lucas, L. V. (2017). What determines water temperature dynamics in the San Francisco Bay-Delta system? *Water Resources Research*, *53*, 9901–9921. https://doi.org/10.1002/2016WR020062

Received 3 NOV 2016
Accepted 26 OCT 2017
Accepted article online 30 OCT 2017
Published online 30 NOV 2017

The copyright line for this article was changed on 24 APR 2018 after original online publication.

Abstract Water temperature is an important factor determining estuarine species habitat conditions. Water temperature is mainly governed by advection (e.g., from rivers) and atmospheric exchange processes varying strongly over time (day-night, seasonally) and the spatial domain. On a long time scale, climate change will impact water temperature in estuarine systems due to changes in river flow regimes, air temperature, and sea level rise. To determine which factors govern estuarine water temperature and its sensitivity to changes in its forcing, we developed a process-based numerical model (Delft3D Flexible Mesh) and applied it to a well-monitored estuarine system (the San Francisco Estuary) for validation. The process-based approach allows for detailed process description and a physics-based analysis of governing processes. The model was calibrated for water year 2011 and incorporated 3-D hydrodynamics, salinity intrusion, water temperature dynamics, and atmospheric coupling. Results show significant skill in reproducing temperature observations on daily, seasonal, and yearly time scales. In North San Francisco Bay, thermal stratification is present, enhanced by salinity stratification. The temperature of the upstream, fresh water Delta area is captured well in 2-D mode, although locally—on a small scale—vertical processes (e.g., stratification) may be important. The impact of upstream river temperature and discharge and atmospheric forcing on water temperatures differs throughout the Delta, possibly depending on dispersion and residence times. Our modeling effort provides a sound basis for future modeling studies including climate change impact on water temperature and associated ecological modeling, e.g., clam and fish habitat and phytoplankton dynamics.

1. Introduction

1.1. Framework

Estuaries are important ecosystems and provide a breeding, feeding, and resting place for species such as birds and fish. Gradients in salinity, water temperature, suspended sediment concentration, vegetation cover, and bathymetry (i.e., tidal flats, and salt marshes) provide unique habitats for an abundance of species. Those gradients may change as a result of human interference (channel deepening, reclamation, damming, and irrigation) and climate change (e.g., sea level rise, increasing air temperatures, changing precipitation patterns, and river flow regimes). The impact of human interferences and climate change on estuarine ecosystems has been the topic of an increasing number of studies (e.g., Bartholow, 1989; Brown et al., 2013, 2016; Cloern et al., 2011; Jeffries et al., 2016; Wagner et al., 2011).

Water temperature is a critical parameter for estuarine ecosystems. Water temperature has a direct impact on the growth rates, presence, and habitat of species (e.g., fish, clams, and phytoplankton) as higher water temperatures can cause stress and even mortality (Brown et al., 2013; Jeffries et al., 2016; Miller & Kamykowski, 1986; Ralston et al., 2015; Swanson et al., 2000; Underwood & Kromkamp, 1999). In addition, water temperature may also impact flow patterns and mixing due to associated density-driven currents and thermal stratification (Monismith et al., 1990, 2006; Sturman et al., 1999). Parameters influencing water temperature are river water inflow (and its temperature), heat exchange with the atmosphere (influenced by solar radiation, cloudiness, humidity, wind, water, and air temperature), heat and water exchange with groundwater and subsoil, and flow interaction with adjacent seas or oceans and the water temperature of those seas and oceans. Climate change is expected to have a considerable impact on most of these parameters and thus on estuarine water temperature and associated ecosystems. An increase in air temperature increases water

temperature. Changes in precipitation will influence runoff, snow cover, timing and amount of snowmelt, cloud cover, and humidity. These changes affect the timing, amount, and water temperature of upstream river discharges into estuaries and influence exchange with the atmosphere directly. Jeffries et al. (2016) performed a data analysis of water temperature during "dry" (2012–2015) and "normal" years (1995–2011) to assess the effect of extreme drought on water temperatures in the Sacramento-San Joaquin Delta. They state that the environmentally relevant exposure temperature of 20°C (a stress threshold for key regional aquatic species) is reached more commonly and earlier in the year during periods of extreme droughts. Assessing the potential effect of climate change scenarios on estuarine water temperatures may help water resource managers to anticipate critical habitat changes and take measures (if possible) which may contribute to conservation of endangered species.

Understanding the relative importance of the drivers of estuarine water temperature is vitally important to estimating the effect of climate change. The effect of changes in these drivers has drawn limited attention in the literature. Monismith et al. (2009) investigated the variation in subtidal temperatures in the tidal San Joaquin River in response to flow rate, dispersion, and heat exchange with the atmosphere by applying an analytical model and heat balance calculations to observed water temperatures. They found that water temperature is significantly influenced by dispersion, and that the dispersion coefficient in the San Joaquin River is much larger than expected for shear flow in rivers. They state that this is a result of the many junctions and the phasing of flows in the Delta channel network. These findings are in agreement with Gleichauf (2015), who highlight the importance of inflows on the water's residence time and hence the time of exposure to atmospheric forcing, as well as the strength of tidal dispersion, on top of the determinative exchange with the atmosphere. In their presentation of a statistical temperature model for the Delta, Wagner et al. (2011) also underscored the importance of exchange with the atmosphere and found that flow rates have a significant effect on the water temperature on shorter time scales, although their correlation between daily-averaged temperature residuals (modeled temperatures minus observed temperatures) and flow rates was low. When temperatures are averaged over a year, however, residuals do correlate with annually averaged flow rates, possibly because high flows push Delta waters seaward and delay, and consequently shorten, the summer peak temperature period (Cloern et al., 2011).

To assess the effect of climate change scenarios on water temperature in the Sacramento-San Joaquin Delta, several studies have been described using statistical models or observations (Brown et al., 2013, 2016; Jeffries et al., 2016; Wagner et al., 2011). Water temperature was decomposed into different signals with individual trends and extrapolated to the future. These studies project that water temperatures will rise (Wagner et al., 2011), the number of high mortality days for the endangered Delta smelt will increase (Brown et al., 2013), and the time available for adult maturation and spawning will decrease (Brown et al., 2016). The approaches of Monismith et al. (2009) and Wagner et al. (2011) have significant skill in reproducing and predicting temperature conditions for the estuary's current state. However, an empirical statistical model based on historically observed temperatures (e.g., Wagner et al., 2011) may not be applicable to a system that is changing structurally. By extrapolating the change in water temperature from the past to the future at individual measurement points using a statistical model, feedback mechanisms and structural changes to the system (e.g., changes to upstream discharge, feedbacks between air temperature, water temperature, and heat fluxes, new diversion structures) are ignored. In addition, observations only provide insight into temperature dynamics at individual locations and cannot provide information at the full spatial scale. We have chosen to implement a process-based model that can calculate water temperatures in response to changing forcing conditions beyond the range of historically observed estuarine water temperatures and local spatial scales. This approach characterizes physics-based responses to new structural configurations, and compute possible feedback mechanisms.

The results of our modeling effort will act as a basis for future modeling (e.g., the CASCaDE project, Computational Assessments of Scenarios of Change for the Delta Ecosystem, http://cascade.wr.usgs.gov/) exploring potential influences of climate and infrastructure change on ecosystem and water quality dynamics in the San Francisco Bay-Delta. For example, Achete et al. (2015) presented 2-D suspended sediment and turbidity dynamics based on the same hydrodynamic model; 3-D suspended sediment modeling will support phytoplankton and fish habitat modeling. This CASCaDE work is carried out within a community modeling effort in which the software, the model, and its input conditions are being made publicly available (www.d3d-baydelta.org and http://californiacoastalatlas.net/). Third parties can run, amend, copy, and distribute the San

Francisco Bay-Delta Model under Creative Commons Attribution-Share Alike 4.0 International License to meet the need for timely and best science.

1.2. Study Area

The Sacramento-San Joaquin Delta is located on the east of San Francisco Bay. We define the "Delta" as the area between Antioch (ANH) and the approximate upstream limit of tidal influence during the dry season (i.e., Sacramento River near Verona and San Joaquin River near Vernalis). The Delta covers an area of about 40 km × 70 km, and consists of a network of river branches and smaller channels that connect the Sacramento River, the San Joaquin River and smaller tributaries to San Francisco Bay and the Pacific Ocean (Figure 1). Water levels in the Delta are influenced by the tide, although the water is mainly fresh. The

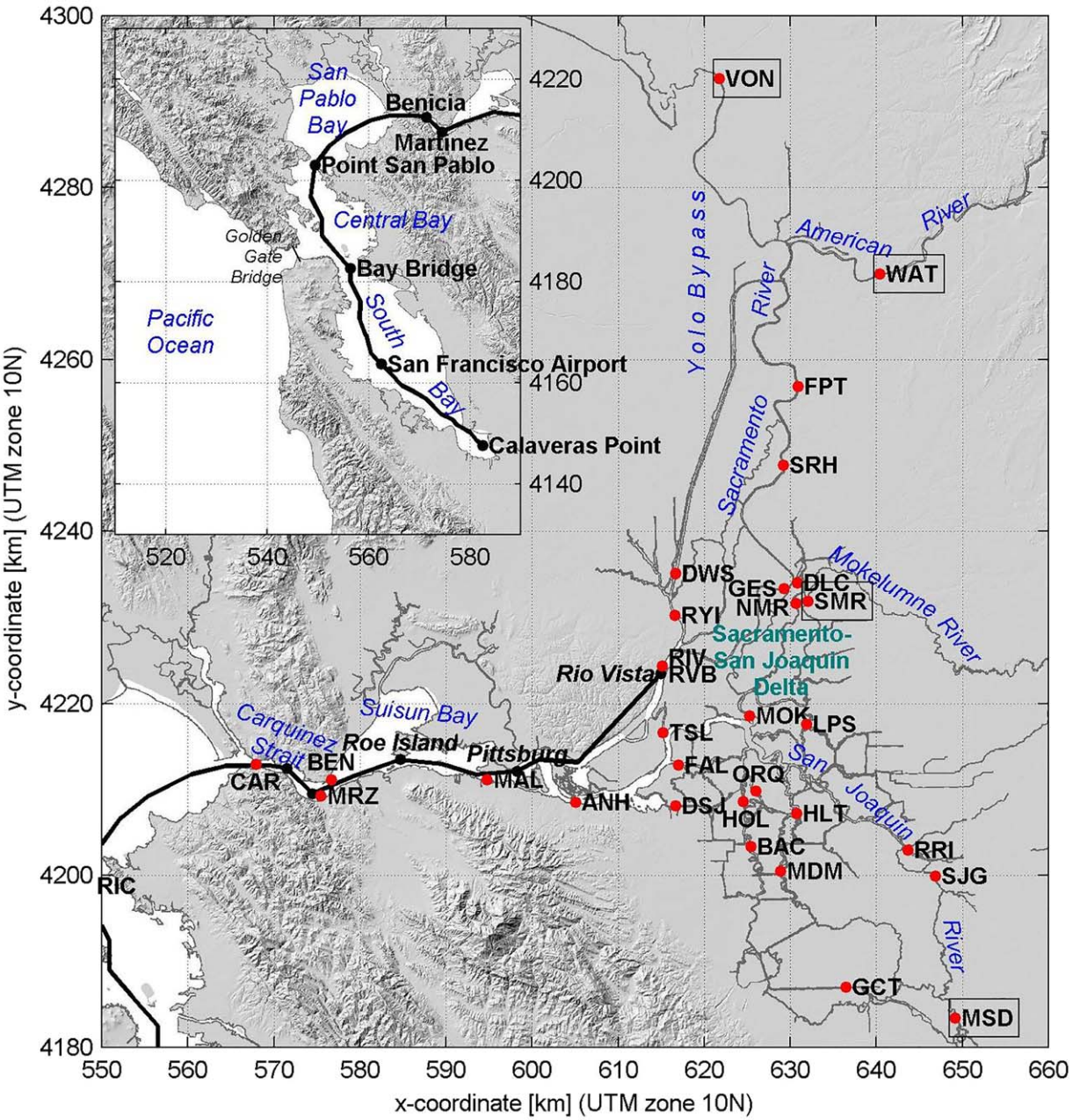

Figure 1. Map of the study area with geographical locations (blue), R/V Polaris cruise track (black line), R/V Polaris stations (black italic text), and time series stations (red dots) with names (black three character codes) in the Delta. Key stations are indicated with a red box, and stations used for boundary conditions are indicated with a black box.

Sacramento River and San Joaquin River are fed by reservoirs located up to approximately 300 to 400 km upstream (Gleichauf, 2015). Reservoir operation thus regulates river flow, although peaks in river flow in winter and early spring (with durations of days to weeks) from precipitation and snow melt are still pronounced. The Sacramento River is the largest supplier of freshwater to the Delta, both directly and via its floodplain, the Yolo Bypass. The discharges of the Sacramento River and the Yolo Bypass together varied seasonally between 300 and 4,500 m^3/s in 2011. River flow not only varies seasonally, but also shows large interannual variations in response to precipitation. The peak daily inflow to the Delta as the sum of gaged and estimated ungaged flows was as low as approximately 1,800 m^3/s in 1992 and more than 15,000 m^3/s in 1997 (Kimmerer, 2002). Water withdrawals also influence flows and salinity intrusion and reached up to approximately 350 m^3/s in 2011. The withdrawals, primarily in the southern Delta, provide drinking water for over 20 million people and irrigation for a multibillion dollar agricultural economy (Brown et al., 2013).

Water management in the Delta serves to safeguard water supply while maintaining ecosystem health. The quantity and timing of water withdrawal is managed to the benefit of irrigation, drinking water supply, and endangered species by, for example, maintaining the position of the salinity gradient in certain locations through reservoir release controls or preventing salmon and other fishes from being entrained by large water pumps via channel and gate closure operations (Grimaldo et al., 2009). The reservoir releases influence both salinity intrusion and water temperatures (Andrew & Sauquet, 2017). Water temperature, salinity, and turbidity are important elements determining the habitat of the endangered Delta smelt (Brown et al., 2013; Swanson et al., 2000). For example, water temperatures higher than 20°C are expected to cause stress for Delta smelt, and high mortality is likely to occur at temperatures over 25°C (Brown et al., 2013; Swanson et al., 2000). Jeffries et al. (2016) state upper thermal tolerances of 27.6°C for Delta smelt and 24.8°C for the endangered longfin smelt. In addition to the water withdrawals, gates, weirs, and barriers divert the flow in specific portions of the year and possibly influence temperature dynamics by altering flow routes and residence times.

The San Francisco Bay-Delta is well-monitored, enabling us to validate our model. The wide temperature variations in this estuary result from mixing of relatively cold ocean water with Delta inflows characterized by seasonally varying temperatures, combined with a wide range of air temperature differences (microclimates); this combination of conditions makes this estuary an interesting case for temperature modeling.

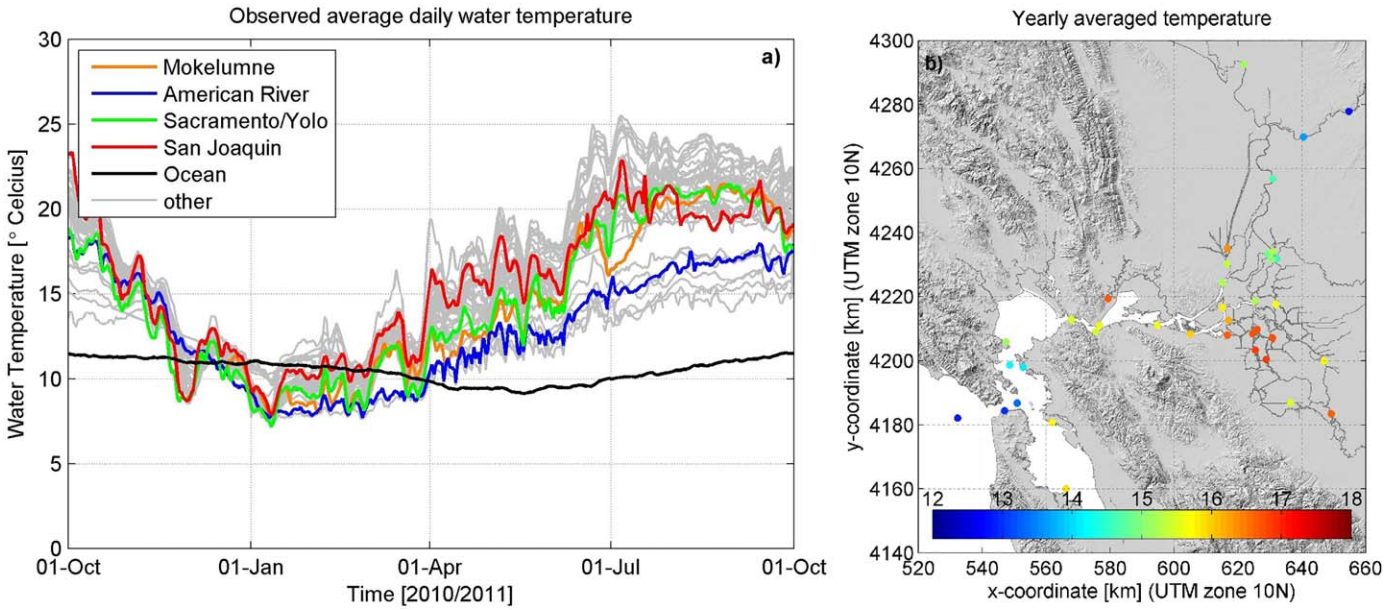

Figure 2. (a) Daily averages of the observed water temperature in the San Francisco Bay-Delta system; at the ocean (ROMS data, black line), near the approximate upstream limits of tidal influence: Sacramento River/Yolo Bypass (VON, green line), American River (WAT, blue line), San Joaquin River (MSD, red line), and Mokelumne River (SMR, gaps filled with VON, orange line), and at other available stations (mainly in the Delta, grey lines) for water year 2011; (b) observed yearly averaged water temperature (2011) for all stations. Data collected from CDEC, CENCOOS, and USGS websites.

Daily-averaged observed water temperatures in the San Francisco Bay-Delta system (Figure 2a) reveal somewhat constant ocean temperatures throughout the year, although temperatures in spring and early summer are a bit lower, probably due to upwelling of cooler water from deeper parts of the ocean. In contrast, stations in the Delta show a clear seasonal variation with temperatures increasing to over 20°C in summer and decreasing to 10°C in winter (grey and colored lines). In winter, the temperature of the ocean is generally higher than the temperature of the stations at the upstream limit of tidal influence (colored lines). The American River in the northeastern Delta is significantly cooler than the other rivers, except in fall, but water temperatures rise when entering the Delta and mixing with warmer Delta water and atmospheric heat exchange takes place (Figure 2b). The southwestern part of the Delta has the highest yearly averaged temperature. In North Bay (consisting of San Pablo Bay, Carquinez Strait, and Suisun Bay), salinity stratification influences the hydrodynamics (Martyr-Koller et al., 2017). During low river flow conditions, salinity intrudes into the confluence of the Sacramento and San Joaquin Rivers near Antioch (ANH), whereas high river flow pulses may shift salinity intrusion tens of kilometers seaward into San Pablo Bay (Jassby et al., 1995).

2. Methods

2.1. Model

We follow a process-based, numerical approach that allows for a close analysis of the relevance of different processes as well as their spatial and temporal variations over the domain. We apply the open source Delft3D-Flexible Mesh software (www.deltares.nl/en/software/delft3d-flexible-mesh-suite/, version 1.1.162.43444) to compute water temperatures for the water years 2011 and 2012. The model of the current study builds upon the model by Martyr-Koller et al. (2017), covering the Sacramento-San Joaquin Delta up to the approximate upstream limit of tidal influence and extending seaward to North Bay, Central Bay, South Bay, and the coastal Pacific Ocean (Figure 3). The unstructured grid consists of approximately 75,000 elements in the horizontal and allows for computation of model results at a spatial resolution down to 10–100 m in the Delta and a time resolution of minutes. The 3-D version of the model has 10 sigma (equidistant) layers in the vertical to capture density-driven currents mainly present in North Bay. The model is publicly available at www.d3d-baydelta.org. The model bathymetry is based on Fregoso et al. (2017) and linearly interpolated onto the grid network. The model is forced with tidal water levels at the ocean based on observations at Point Reyes (www.tidesandcurrents.noaa.gov). Locations of Delta pumps, gates, barriers, and weirs included in the model are indicated in Figure 3 and their operations are provided by California Department of Water Resources. The bed roughness is prescribed with the Manning coefficient and has been varied as part of the extensive calibration and validation of water levels, discharges, and salinity dynamics and stratification for the wide-ranging tidal and fluvial conditions during water years 2011 and 2012 by Martyr-Koller et al. (2017). The Manning coefficient varies between 0.015 $s/m^{1/3}$ in the channels of North Bay and 0.033 $s/m^{1/3}$ in the eastern part of the Delta. Also the viscosity and diffusivity parameters were chosen based on the hydrodynamic and salinity calibration, and have not been part of the temperature calibration.

Thermal inputs to the Delta from multiple rivers, not all of which were directly measured, either use the measured temperature of that river or a proxy temperature from a nearby river. The rivers and the temperature station used (in parentheses) are Sacramento River (VON), American River (WAT), San Joaquin River (MSD), Mokelumne and Cosumnes River (SMR, gaps filled with VON), the Yolo Bypass (VON), Napa River (VON), Sonoma River (VON), and Petaluma River (VON). Locations are shown in Figure 1. Depth-constant temperature at the ocean boundary was prescribed with output from the Regional Ocean Modeling System model suite (ROMS) (Neveu et al., 2016).

The Ocean Heat Flux Model functionality of Delft3D-FM was activated to account for atmospheric heat exchange. The heat flux model requires input of relative humidity, air temperature, cloudiness, and wind. To ensure good spatial coverage, we use daily inputs of humidity and net incoming short wave radiation based on the METDATA data set (Abatzoglou, 2011). METDATA's specific humidity and shortwave radiation are used in combination with the Livneh air temperature data set (Livneh et al., 2015). The METDATA and Livneh data sets cover the entire model domain, except the centers of Central and South Bay and the ocean. The bays are filled with linear interpolation from the METDATA and Livneh data sets. Air temperature above the ocean uses the observed values from the NOAA station at Half Moon Bay (46012), while for humidity

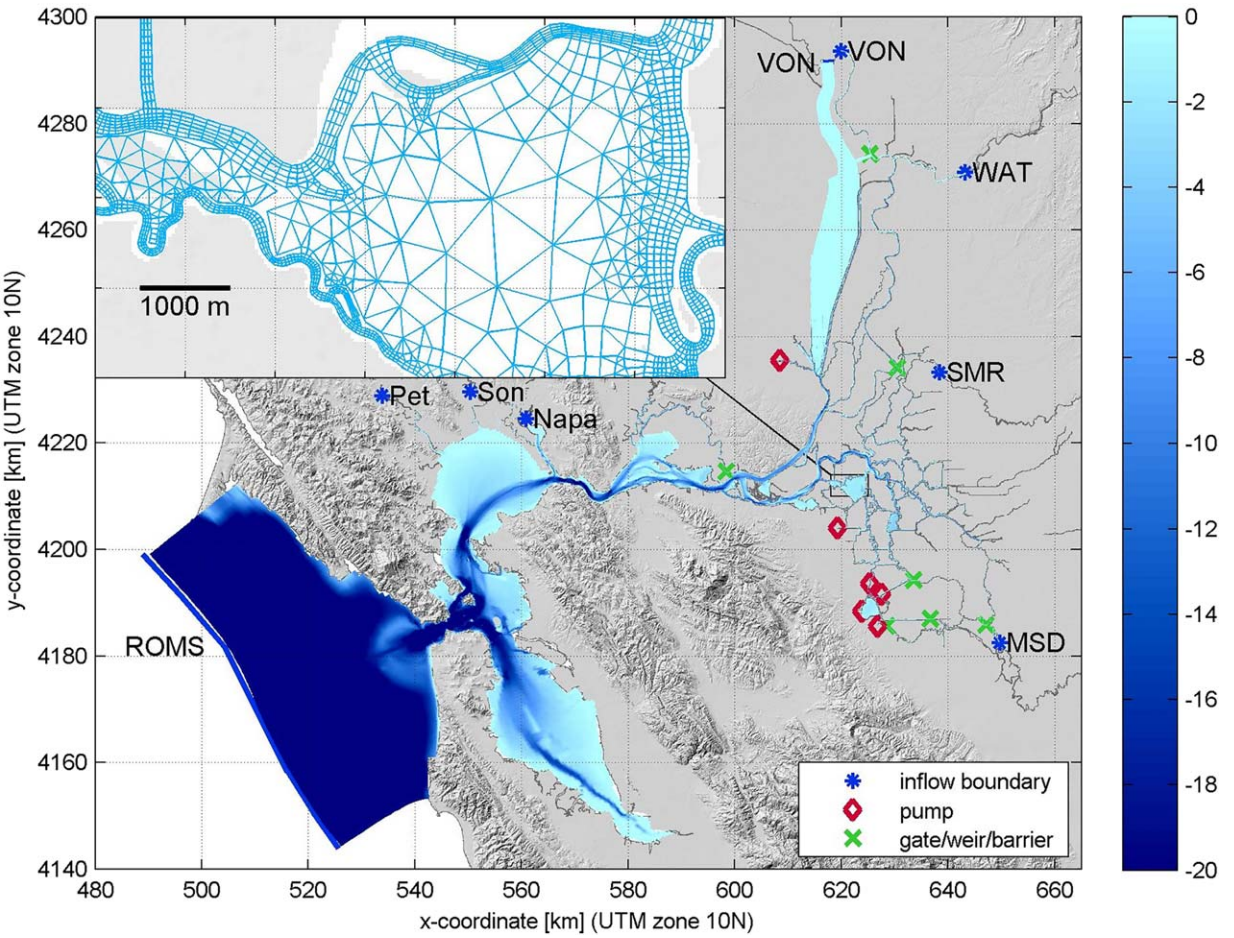

Figure 3. Model bathymetry with inset showing grid resolution. Dark blue symbols and lines indicate inflow boundaries, red diamonds show pumps and green crosses point out gates, weirs and barriers.

the METDATA value at Point Reyes is used. The data are projected on an equidistant grid with a mutual distance of 5 km. Hourly values of the relative humidity are computed from the average daily specific humidity using the air temperature and a constant atmospheric pressure of 1,013 kPa (see Appendix A). The maximum and minimum daily air temperatures were used to derive hourly values by assuming the maximum temperature occurs at 4 PM and the minimum temperature occurs between midnight and 5 AM. For the remaining time, a sine function is fitted (see Appendix A). The daily-averaged downward shortwave radiation was used to determine the cloudiness, i.e., the percentage of the sky covered with clouds. The model computes clear-sky solar radiation for any location on earth using the latitude and the Julian day. The cloudiness follows from the clear-sky solar radiation at ground level and the downward solar radiation at ground level (see Appendix A).

The model is forced with spatial wind fields on an equidistant grid with a cell size of 1.5 km obtained from an interpolation of observed hourly wind data from approximately 40 stations throughout the study area, taking into account the topography (Ludwig & Sinton, 2000).

The model simulations are started with an initial salinity field that decreases gradually from the ocean (approximately 33.5 ppt) to the freshwater inflow boundaries. The initial water temperature is 15°C over the entire domain. The model is run for 2 months to spin-up salinity and temperature and the subsequent 24 months are used in the analyses.

After investigation of the importance of thermal stratification (see section 3.1), sensitivity runs were executed with a depth-averaged version of the model, only focusing on the Delta. This allowed us to execute a large number of sensitivity tests at low computational cost.

2.2. Data Sources

Time series of observed water temperatures at stations (Figure 1) throughout the San Francisco Bay and Delta region were collected from the California Department of Water Resources (DWR, M. Dempsey, personal communication, 2016), CDEC (http://cdec.water.ca.gov/), CENCOOS (data.cencoos.org), and USGS (waterdata.usgs.gov/) websites and were used for model calibration and validation, as well as for boundary conditions. When the vertical position of the temperature sensor in the water column was reported, the station was used for calibration of the 3-D model. Stations missing this information were used for validation of the 2-D model. The time series were thinned to an hourly time interval and small gaps (<3 h) were filled by linear interpolation.

During approximately monthly cruises of the USGS Research Vessel Polaris (Cloern & Schraga, 2016; Schraga & Cloern, 2017), the water temperature was measured while sailing from South Bay (Calaveras Point) to the Delta (Rio Vista). The Polaris temperature transects (Figure 1) discussed herein are based on vertical profiles of observed water temperature at individual stations at different times, which have been interpolated linearly and compared to model output.

We use specific key stations (red box stations in Figure 1) in distinct areas to investigate model performance and temperature dynamics in detail. The Martinez (MRZ) and Rio Vista (RVB) stations and the Polaris cruises are used to analyze 3-D dynamics and the influence of salinity in North Bay. Station Rough and Ready Island (RRI) near Stockton is located in a deep part of the San Joaquin River, making it suitable for analysis of thermal stratification in the Delta. The Southwest Delta is relatively far from the model boundaries and is analyzed using station Bacon Island (BAC). Station Little Potato Slough (LPS) is chosen for its location in the center of the Delta.

2.3. Model Calibration

We calibrated the model in 3-D against observed temperatures for water year 2011 (1 October 2010–30 September 2011). The model calibration for temperature was done by increasing the accuracy of the model input, varying Stanton and Dalton numbers (for fine-tuning the convection of heat by wind, increasing or decreasing the water temperature over the entire year) and changing the Secchi depth (influencing the absorption of heat in the water column). For the Stanton and Dalton numbers and the Secchi depth, the default values turned out to be the best settings. We improved the model performance significantly by changing from spatially uniform relative humidity, air temperature, cloudiness, and wind speed measured at Stockton to spatially varying values. Changing the sea boundary from observed sea surface temperature at Point Reyes to depth-averaged water temperature obtained from a ROMS ocean model (Neveu et al., 2016) also better reproduced the observed water temperatures due to large vertical water temperature differences in the ocean.

Table 1
Bias, RMSE, R^2 of 3-D Model for Water Year 2011 and 2012

	2011			2012		
	Bias (°C)	RMSE (°C)	R^2 (–)	Bias (°C)	RMSE (°C)	R^2 (–)
ANH lower	0.15	0.75	0.99	0.01	0.91	0.99
ANH upper	0.05	0.83	0.99	0.00	0.86	0.99
BAC	−0.28	0.85	0.99	−0.23	1.10	0.99
BEN lower	−0.12	0.95	0.96	0.80	1.40	0.99
BEN upper	0.07	1.14	0.98	0.40	1.47	0.98
CAR lower	0.21	0.86	0.98	0.37	0.84	0.97
CAR upper	0.25	0.86	0.98	0.10	0.83	0.98
FAL	0.10	0.86	0.99	0.00	0.93	0.99
MAL lower	0.21	0.92	0.99	0.18	1.10	0.99
MAL upper	0.14	0.93	0.99	0.24	1.09	0.99
MOK	0.02	0.70	0.99	−0.25	0.71	0.99
MRZ lower	0.58	1.04	0.98	0.32	1.24	0.98
MRZ upper	0.15	0.98	0.98	0.43	1.35	0.98
RIC lower	0.16	0.71	0.94	0.26	0.68	0.95
RIC upper	0.08	0.75	0.93	0.30	0.79	0.91
RRI lower	−0.45	0.77	0.98	−1.06	1.20	0.99
RRI upper	−0.80	1.12	0.98	−1.10	1.23	0.99
RVB	0.16	0.82	0.99	−0.10	0.77	0.99
SMB lower	0.26	0.87	0.97	0.46	1.16	0.97
SMB upper	0.20	0.82	0.98	0.45	1.13	0.97
SRH	0.09	0.63	0.99	−0.03	0.62	0.99
TSL	0.18	0.88	0.99	0.07	0.90	0.99

The bias (difference between time-averaged modeled and time-averaged observed values), root mean square error, and coefficient of determination (R^2) were computed to compare the observed and modeled water temperatures for the entire WY2011 in 3-D mode (Table 1). The bias varied spatially between −0.8°C and 0.58°C. Both positive and negative values of the bias indicate that there was no structural overestimation or underestimation of the modeled temperature over the entire model domain. The majority of stations have an RMSE smaller than 1°C. The high R^2 (>0.9) indicates that the phasing of the temperature variation is well reproduced by the model.

Figure 4 shows a target diagram (Jolliff et al., 2009) for the model performance of water temperature for the 3-D model for WY2011 (black dots) and WY2012 (blue triangles). The unbiased RMSE (uRMSE, horizontal axis) and the bias (vertical axis) are visualized for each station. Both the bias and the uRMSE have been normalized with the standard deviation of the observations, in order to objectively evaluate model

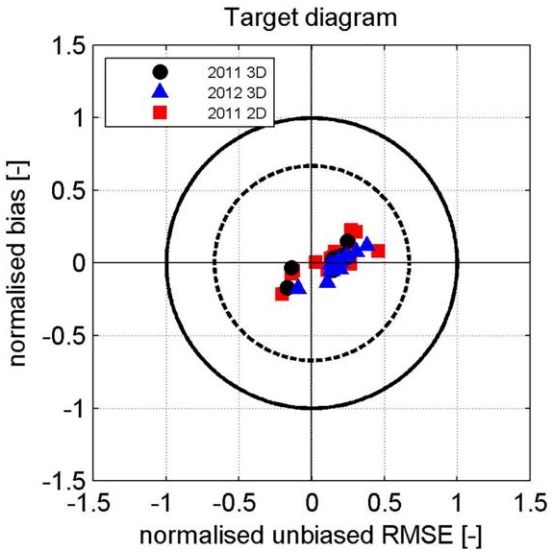

Figure 4. Target diagram for comparing modeled and observed water temperatures for the 2011 (black dots) and 2012 (blue triangles) 3-D model results and the 2011 2-D model results in the Delta (red squares).

performance and possibly compare with other parameters (e.g., Martyr-Koller et al., 2017). The distance to the origin gives the RMSE (including bias) and smaller distance reflects better model performance. Points within the unit circle indicate good model performance (Jolliff et al., 2009). The model showed good performance for 3-D calibration and validation, with all points falling within the unit circle. Modeled temperatures had a wider standard deviation than observations (RMSE $>$ 0) for many locations. Normalized bias was positive and negative for both calibration and validation years, indicating no systemic temperature bias at the annual scale. The model performance of the 2-D model (red squares in Figure 4) is discussed in section 3.1. Figures with time series of observations and model outputs for individual stations can be found in supporting information.

Figure 5 shows the observed and computed water temperature for stations Rio Vista Bridge (RVB) and Bacon Island (BAC) in the Delta. The model captures the seasonal variations, but has a tendency to slightly under predict temperatures in winter and over predict in summer in the entire model domain. The better match between computed water temperatures and measurements in spring may be related to the strong signal from the model boundaries, as the total river discharge is highest in spring (up to 5,600 m^3/s in 2011). Figure 6 shows that the daily variation is also captured by the model, although the magnitudes can deviate from the observed water temperature.

Model output is generated at approximately the same locations and times as the R/V Polaris measurements, for each of the 10 vertical layers. Figure 7 shows the observed and modeled vertical profiles for the June

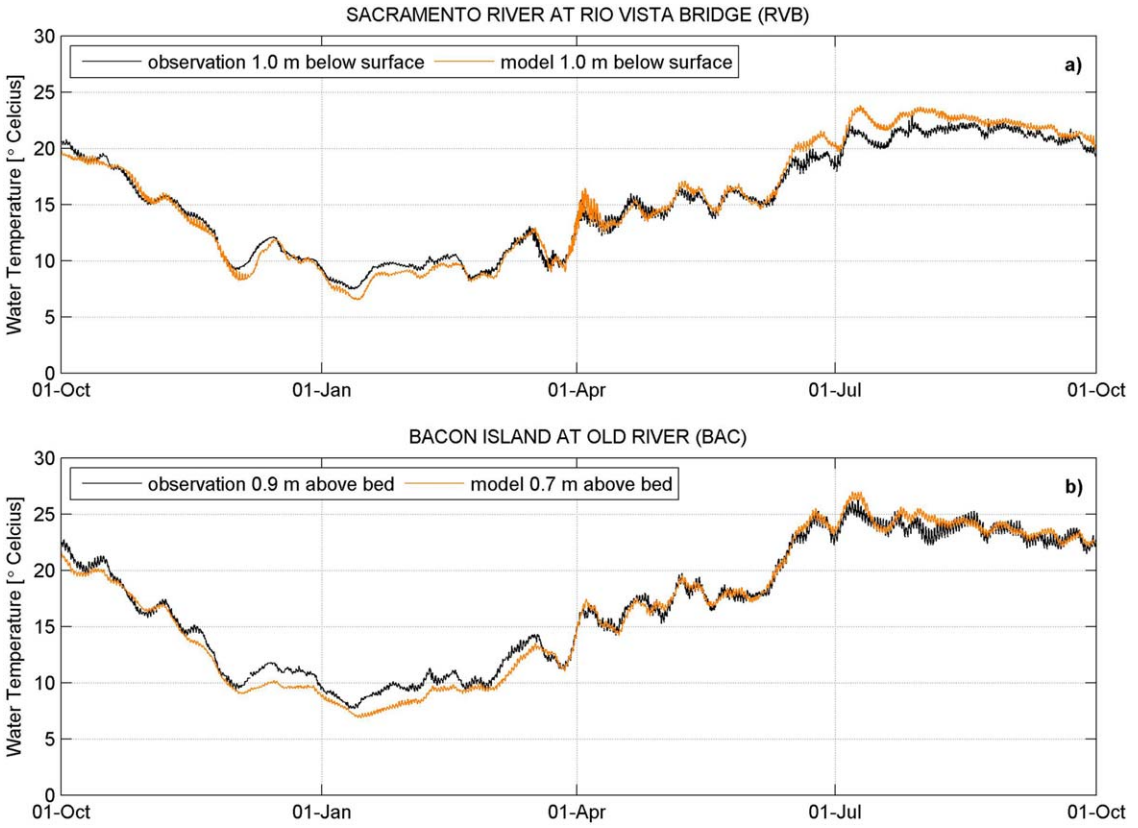

Figure 5. Observed (black) and computed (orange) water temperature at station (a) Rio Vista Bridge and (b) Bacon Island for water year 2011 with the 3-D model.

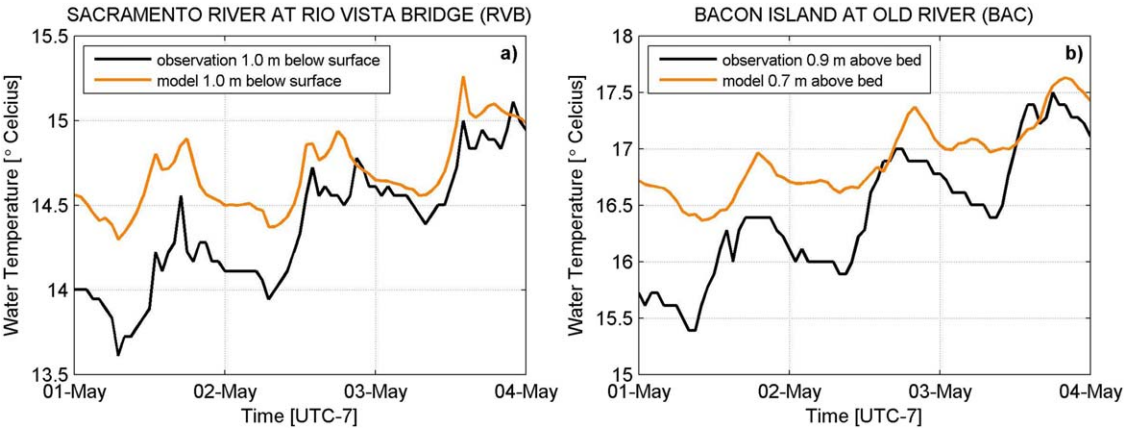

Figure 6. Observed (black) and computed (orange) water temperature at stations (a) Rio Vista Bridge and (b) Bacon Island at Old River for 3 days in May 2011.

2011 cruise. (Figures of cruises on other dates are included in supporting information.) The model captures the temperature throughout the domain (Figures 7a and 7b), with the temperatures near the Golden Gate Bridge (between Bay Bridge and Point San Pablo) being the lowest, as a result of the inflow of cold ocean water. Between Point San Pablo and Martinez, both the Polaris transect and the model show thermal stratification. Model agreement with observations was poorer in South Bay, probably as a result of the coarse grid resolution, exclusion of local tributary flows, and no hydrodynamic model calibration for that specific area. Figures 7c and 7d show the impact of salinity dynamics on temperature in North Bay. Removal of salinity dynamics leads to less thermal stratification between Point San Pablo and Martinez, and warmer temperatures throughout Central, San Pablo, and Suisun Bays. This is described in further detail in section 3.1.

Without extensive calibration and with relatively coarse forcing conditions (5 km grid resolution for the atmospheric forcing, schematized air temperature cycle over the day) we obtained biases for the different time series stations between −0.8°C and 0.58°C, RMSE's below 1.15°C, and coefficients of determination R^2 above 0.92 for WY2011 (see Table 1) implying that the model is robust and can be used to assess effects of changing forcing conditions.

2.4. Model Validation

After calibration of the temperature for water year 2011, we validated the model for water year 2012, applying the same forcings schematization, and settings. Water year 2011 is considered a "wet" year, with a peak river inflow of approximately 5,600 m^3/s. We validated the model for a "below normal" year with respect to peak river inflow to evaluate the model performance under different hydrodynamic conditions. Water year 2012 had a peak river inflow of approximately 1,500 m^3/s. The 2012 model validation shows model performance values that are comparable to 2011 (Table 1 and Figure 4), but with slightly larger biases (between −1.1°C and 0.8°C) and RMSE (between 0.62°C and 1.47°C) than 2011. As such, we are confident that our model can accurately predict water temperatures under both low and high flow conditions.

2.5. Sensitivity Tests

We investigated the importance of different drivers of water temperature in the Delta: different terms in the meteorological forcing (humidity, air temperature, and cloudiness), the water temperature of the inflowing rivers and the ocean, and the discharge of upstream rivers. The effect of inflow temperature on Delta water temperatures was studied by adding 2°C to all inflow temperatures used in the reference (validated WY2011) simulation. Separately, the effect of a change in ocean temperature was explored by increasing that boundary condition by 2°C relative to the reference temperature. The effect of the atmospheric forcing within the Delta was investigated by switching off the heat flux model and only allowing for transport of temperature. A simulation with reduced discharge was also performed to explore the effect of velocities and residence times.

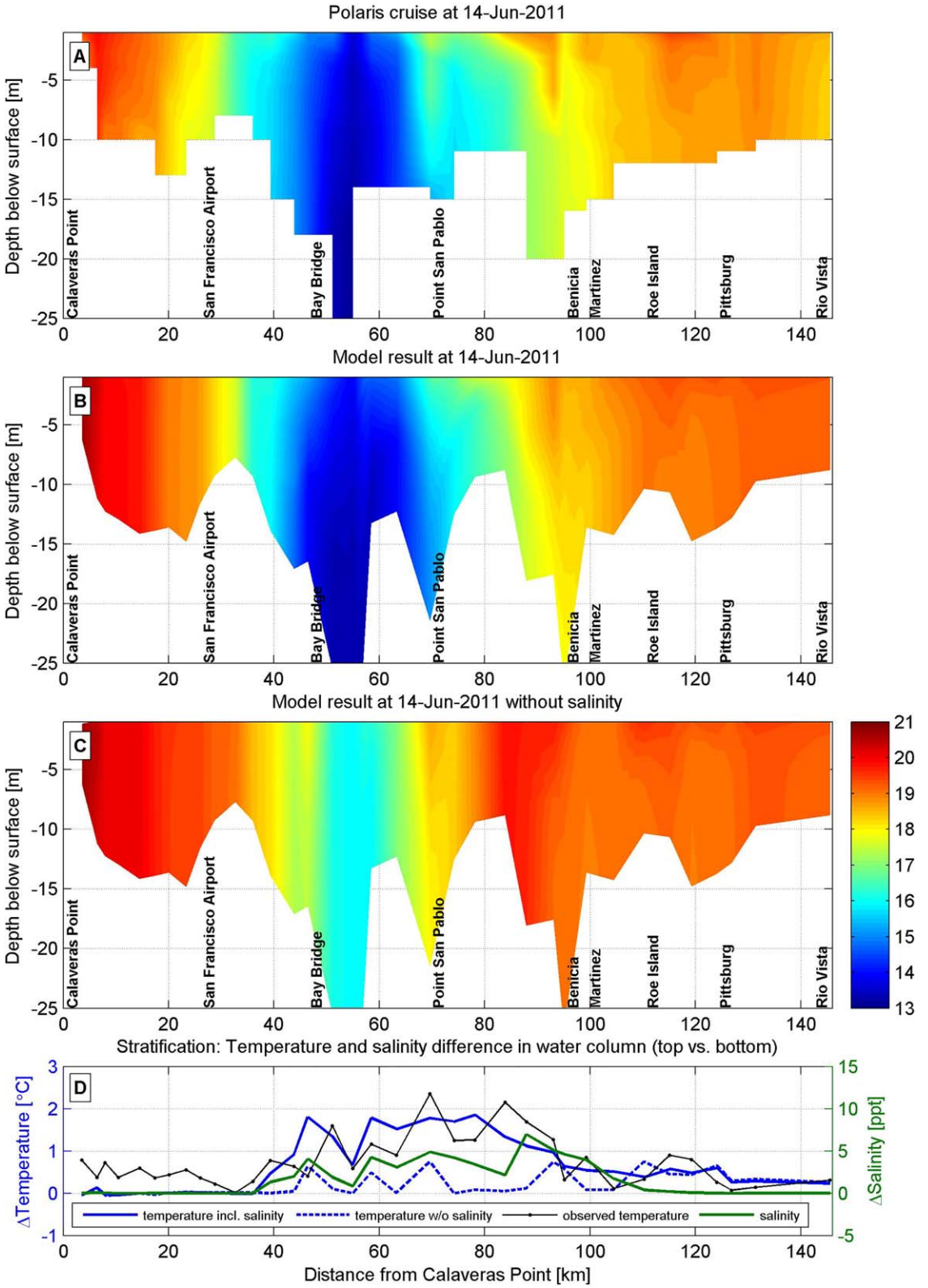

Figure 7. Comparison of water temperature (a) observed during the R/V Polaris cruise of 14 June 2011, (b) the corresponding model result, (c) the model result without salinity taken into account, and (d) the difference between near-surface and near-bed temperature (left axis) for model result with salinity (corresponding to Figure 7b, blue solid line), model result without salinity (corresponding Figure 7c, blue dashed line), the modeled salinity stratification (green line, right axis), and the observations (corresponding to Figure 7a, black line).

3. Results

3.1. Importance of Thermal Stratification

Observations show that thermal stratification is present at some locations in our area of interest, for instance, in Central and North Bay (between Bay Bridge and Pittsburg in Figure 7). This stratification is strongest approximately between Bay Bridge and Benicia, and is well captured by the model including salinity (Figure 7b), indicating that in this area 3-D interaction of salinity and temperature dynamics are important. Figure 7c shows the model result for a simulation without salinity, which produces warmer temperatures and less stratification in North Bay than Figure 7b. This indicates that salinity gradients enhance intrusion of both salt and cool ocean water into the estuary. The Martinez Station (Appendix A) has two sensors in the water column, one close to the surface and one close to the bed. Although the model reproduces some thermal stratification, it under predicts the temperature variation over the water column at this station. Upstream of Pittsburg, the importance of salinity dynamics seems to diminish. Thermal stratification is coupled to salinity intrusion as the largest temperature differences over the water column coincide with salinity stratification (Figure 7d). Some pure thermal stratification is present between Roe Island and Rio Vista, where modeled salinity stratification is absent (Figure 7d).

As salinity stratification is generally absent in the Sacramento-San Joaquin Delta, it does not drive thermal stratification there. Thermal stratification may occur in the west Delta, as shown by R/V Polaris observations at Rio Vista (Figure 8). During some periods, the stratification is also captured by the model. Both in the model and the measurements, the stratification occurs limitedly and occasionally and is not persistent in time. Station Rough and Ready Island, (RRI) near Stockton, is located in a relatively deep portion of the San Joaquin River in the east Delta. Observations show persistent thermal stratification here (Figures 9c and 9d), which is strongest during the afternoon as a result of atmospheric forcing (air temperature, Figure 9a). The model reproduces the thermal stratification in the afternoon, when both in the model and the observations the temperature difference over the water column is largest (Figure 9d), but during the night stratification is underestimated. During decreasing air temperatures (and solar radiation) in the evening and related reduced thermal stratification, (modeled) tidal depth-averaged peak velocities of 20 cm/s (Figure 9b) mix water thoroughly, resulting in depth-uniform temperatures and an (temporal) increase of near-bed temperatures. During increasing air temperatures (and solar radiation) thermal stratification develops, which hampers the mixing by the tidal currents of 20 cm/s. In observations, the thermal stratification is maintained during the night, implying weaker mixing than in the model. This suggests that decreasing vertical diffusivity (by adapting the diffusion coefficient or applying a z-layer model instead of the current σ-layer model), may enhance model results, at least for the dynamics at this particular station and

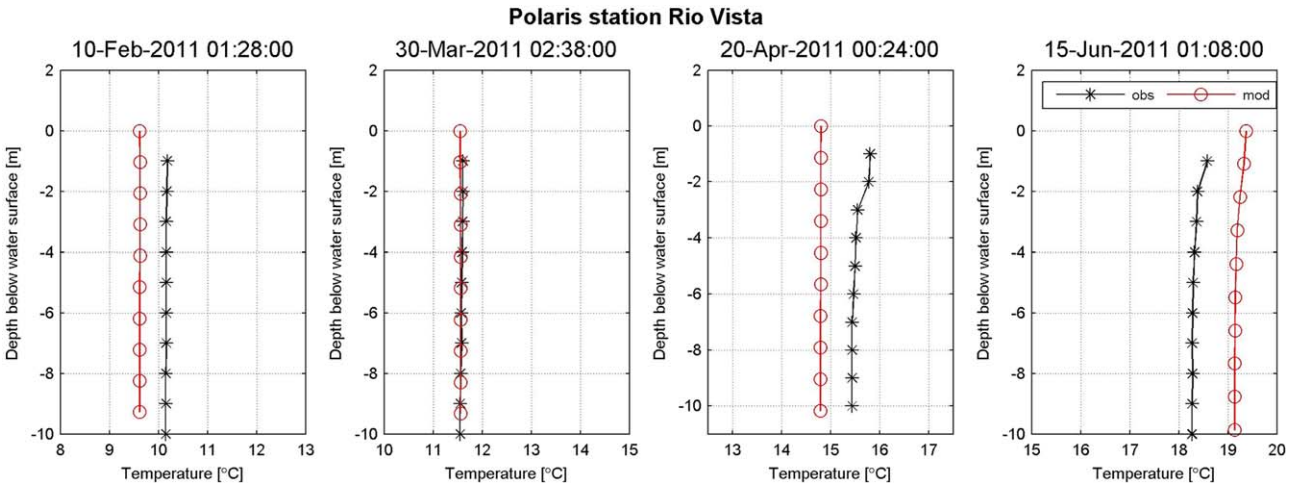

Figure 8. Observed (black) and computed (red) water temperature over the water column at Polaris location P657 near Rio Vista Bridge at 10 February, 30 March, 20 April, and 15 June.

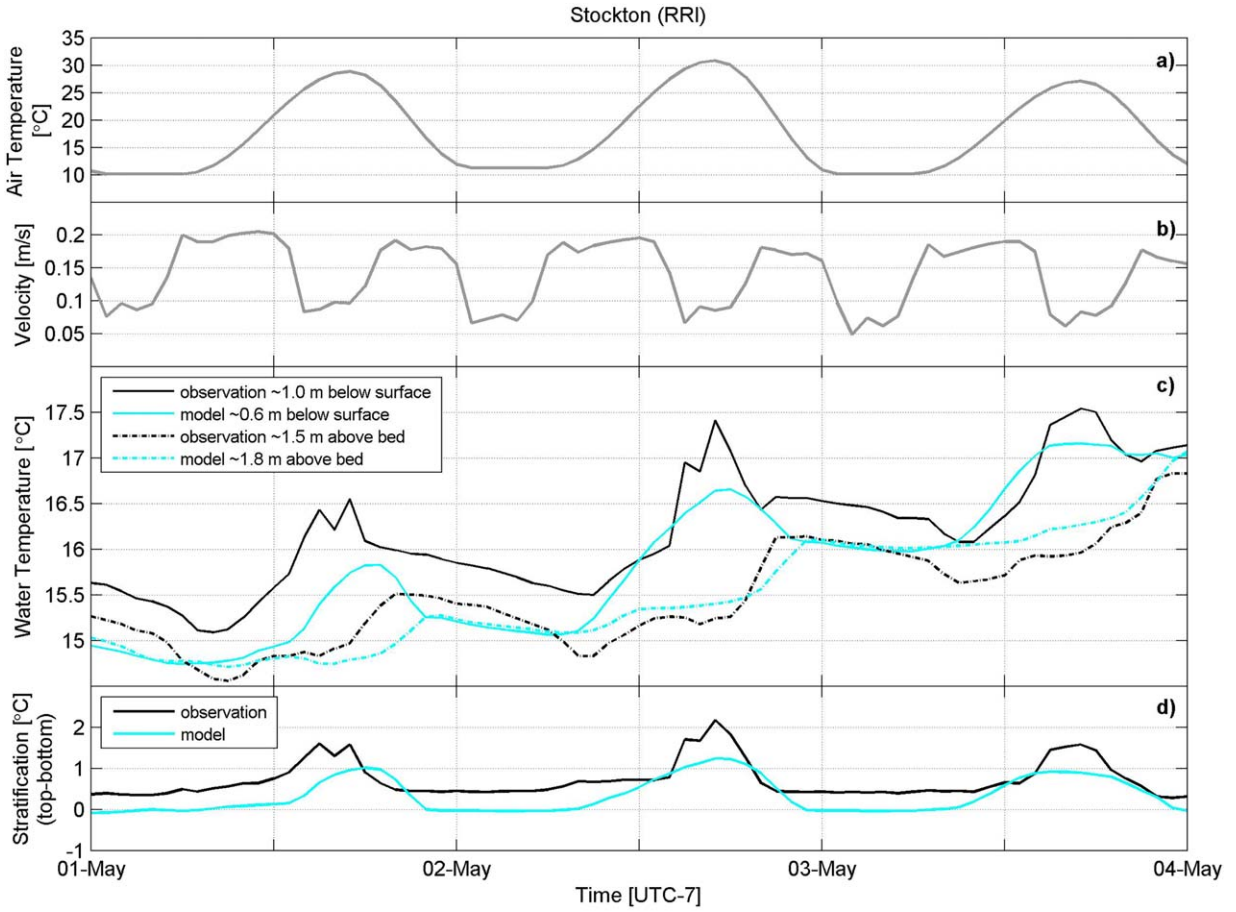

Figure 9. (a) Air temperature, (b) modeled depth averaged velocity, and (c) observed water temperature at the surface (black) and near the bed (blue) and computed water temperature at the surface (orange) and near the bed (cyan), at station Rough and Ready Island (RRI) near Stockton for 3 days in May 2011.

during this period of time. Although the dynamics of model results and observations show similar trends, it is important to note that intradaily temperature variations and vertical temperature differences are similar to the bias between model results and observations of −0.8°C in Table 1.

Most temperature time series stations provide observations for a single position in the water column, and do not measure stratification. We know that thermal stratification occurs in North Bay, where it is enhanced by salinity stratification, and near Stockton and Rio Vista, where the water depth is relatively large. The model most closely reproduces thermal stratification in areas impacted by salinity-driven gradients such as North Bay, and to a lesser extent in freshwater deep channel locations with persistent stratification such as Stockton. Although the modeled thermal stratification magnitude is usually weaker than in observations in areas where purely thermal stratification occurs, the model reproduces similar stratification dynamics at these locations (Figure 9d). Hence, we can use the model to explore whether thermal stratification is present at other (one sensor) observation stations. For the maximum temperature difference in the water column, the mean value, and the mean of the 5% highest values can be computed (Figure 10). Thermal stratification is largest in Central and San Pablo Bays, and also large in South Bay and Carquinez Strait. The smallest values are obtained for the Delta (black dots close to the origin in Figure 10). Hence, our model suggests that thermal stratification is least important in the Delta, where values for the mean differences are typically smaller than 0.2°C. Stations RRI, GCT, and DLC occasionally show larger differences, as is shown by the mean of the 5% largest values. Larger modeled thermal stratification at RRI agrees with observations (Figure 9). Stations Delta Cross Channel (DLC) and Grantline Canal at Tracy Road Bridge (GCT) are located close to barriers, which may strongly affect the local velocities and hence mixing and temperature dynamics.

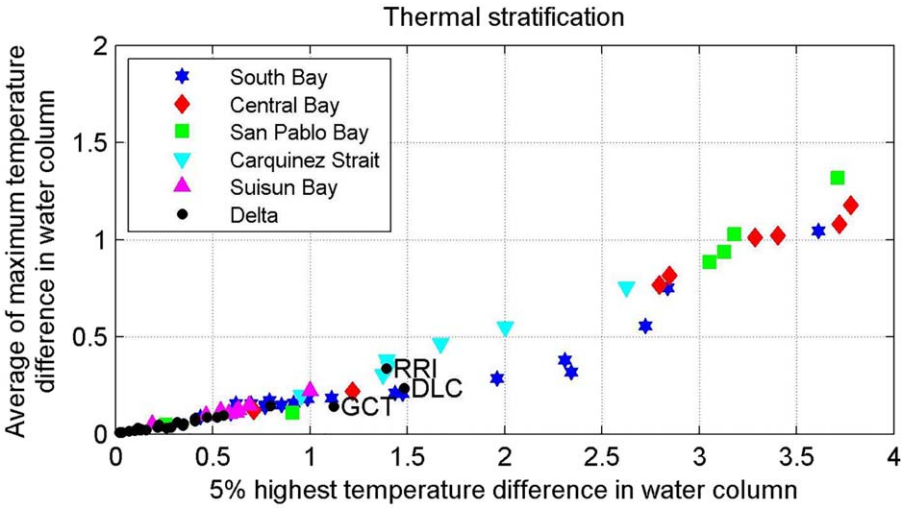

Figure 10. Mean (vertical axis) and mean of the 5% highest values (horizontal axis) of the modeled temperature difference over the water column per station in the 3-D model for water year 2011. Black dots represent stations in the Delta, colored markers are stations in other areas (see legend).

As thermal stratification does not appear widespread in the Delta, this region may also be studied using a depth-averaged (2-D) version of our model to save computational cost. The bias, RMSE, and coefficient of determination for stations in the Delta are listed in Table 2 for the 2-D version of the model. The model statistics have also been visualized in Figure 4. Again, stations GCT, DLC, and RRI show larger biases and RMSE values than most other stations in the Delta. Skill metrics for the common 3-D and 2-D stations did not change much between the 2-D and 3-D versions of the model (Tables 1 and 2), and Figure 10 shows that for most delta stations stratification is on average very weak.

Table 2
Bias, RMSE, R^2 of 2-D Model for Water Year 2011 for Stations in the Delta

	Bias (°C)	RMSE (°C)	R^2 (–)
ANH lower	0.18	0.77	0.99
ANH upper	0.09	0.85	0.99
BAC	−0.27	0.86	0.99
DLC	0.36	2.11	0.91
DSJ	−0.04	1.41	0.98
DWS	0.25	1.12	0.98
FAL	0.12	0.88	0.99
FPT	0.14	0.58	0.99
GCT	0.52	1.20	0.95
GES	0.04	0.61	0.99
HLT	−0.17	0.67	0.99
HOL	−0.13	0.97	0.99
LPS	0.19	0.99	0.98
MDM	−0.27	0.63	0.99
MOK	−0.02	0.68	0.99
NMR	0.37	0.86	0.98
ORQ	−0.11	0.91	0.99
RIV	0.30	0.87	0.99
RRI lower	−0.34	0.69	0.98
RRI upper	−0.99	1.36	0.97
RVB	0.15	0.83	0.99
RYI	0.18	0.99	0.99
SJG	−0.25	0.60	0.99
SRH	0.07	0.62	0.99
TSL	0.14	0.86	0.99

3.2. Delta Water Temperature Sensitivity Based on a 2-D Model

Figure 11 shows the modeled effects of changes in the different drivers on water temperature in the Delta, computed with the 2-D model. A 2°C increase in inflowing river temperature (Figure 11a) has a substantial impact on water temperatures in most of the Delta. The effect is strongest near the inflow points and decreases toward Antioch (ANH). The southwestern Delta, i.e., the area around Bacon Island at Old River (BAC), is affected less. The effect of a warmer ocean (Figure 11b) has a negligible effect on water temperature in the Delta as oceanic water equilibrates with atmospheric conditions before entering the Delta.

Figure 11c shows the effect of the atmospheric heat forcing. In almost the entire Delta the exchange of heat with the atmosphere results in higher average temperatures. This effect is again strongest in the southwestern Delta. In the southeastern part of the Delta, where the San Joaquin River enters the model domain, the water temperature is (on average) lowered when we allow for heat exchange with the atmosphere.

When the discharge of the inflowing rivers is reduced to 33% of the discharge in the reference simulation (Figure 11d), comparable to the difference in peak discharge between WY2011 and WY2012, the temperature rises in almost the entire Delta with increases up to 1°C averaged over the year. This rise is largest in the central Delta, around stations Little Potato Slough at Terminous (LPS) and Mokelumne River at San Joaquin River (MOK).

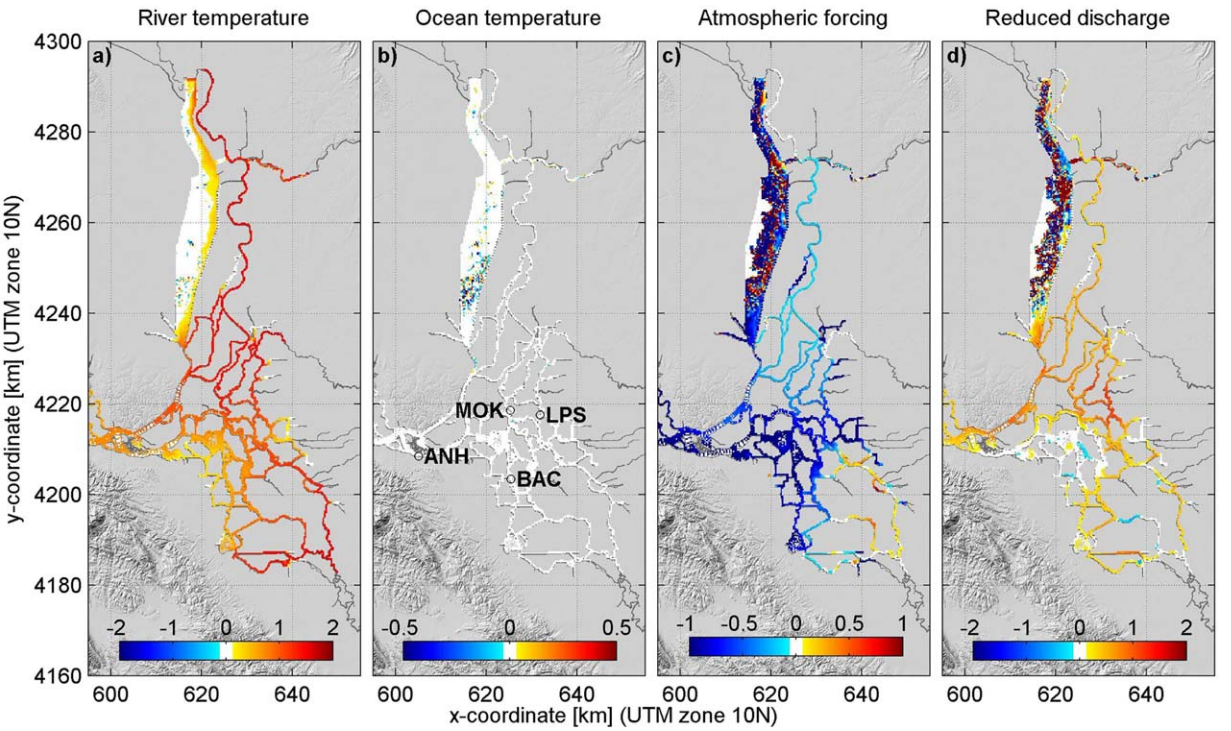

Figure 11. Yearly average water temperature difference with respect to the 2-D reference simulation for water year 2011 for (a) an increase of the inflowing river temperature of 2°C, (b) an increase of the ocean temperature of 2°C, (c) switching off the heat flux model, and (d) reducing the river discharge to 33% of the reference simulation. Note color bar limits vary between the plots.

Quite large differences can be observed in the very shallow and alternately drying and flooding areas such as the Yolo Bypass (Figure 11). These results should be ignored, because the heat flux model is not accurate in very shallow, regularly dry areas (such as the Yolo Bypass or intertidal flats) due to the removal of excess heat from the water column instead of taking into account heat exchange with the subsoil.

The relative importance of each of the drivers appears dependent on the local hydrodynamics and residence times. Although residual velocity does not capture all potentially important processes (e.g., tidal dispersion; Monsen et al., 2002) influencing residence time, here we use residual velocity as an indicator of residence time. Figure 12a shows the modeled depth-averaged residual velocity for WY2011 for various stations in the (tidal) Delta and indicates that large residual velocities are close to the inflow boundaries. We infer that these larger residual velocities result in a relatively large effect of the river inflow temperature and confine the atmospheric forcing to a relatively small effect. In contrast, small residual velocities are present in the southwestern Delta, near BAC, compared to other stations, which make this region probably more susceptible to atmospheric forcing. The residual velocity in this area is hardly affected when the discharge is strongly reduced (Figures 12b and 12c), resulting in a negligible effect of changes in discharges on the water temperature. The decrease in residual velocities in the central Delta (Figure 12c) may allow for more exchange with the atmosphere, resulting in a higher average water temperature.

Averaged over a year, some of the drivers showed quite a large impact (Figure 11). On shorter time scales, or in different seasons, the impact was even bigger. Indeed, at station BAC, the impact of the atmospheric forcing on modeled temperature is very large (Figure 13), while other drivers have a relatively small impact. The difference as a result of atmospheric forcing can reach 10°C in summer. At station Little Potato Slough at Terminous (LPS), the impact of the atmospheric heat flux is much lower than at BAC and the effect of the increased river inflow temperature, atmospheric forcing, and discharge volume all have impacts on the same order of magnitude. Consequently, water temperature differences do not exceed a 5°C with respect to the reference simulation. At this station, the atmospheric forcing has less impact; we hypothesize that shorter residence times at LPS relative to BAC contribute to the smaller influence of atmospheric forcing at

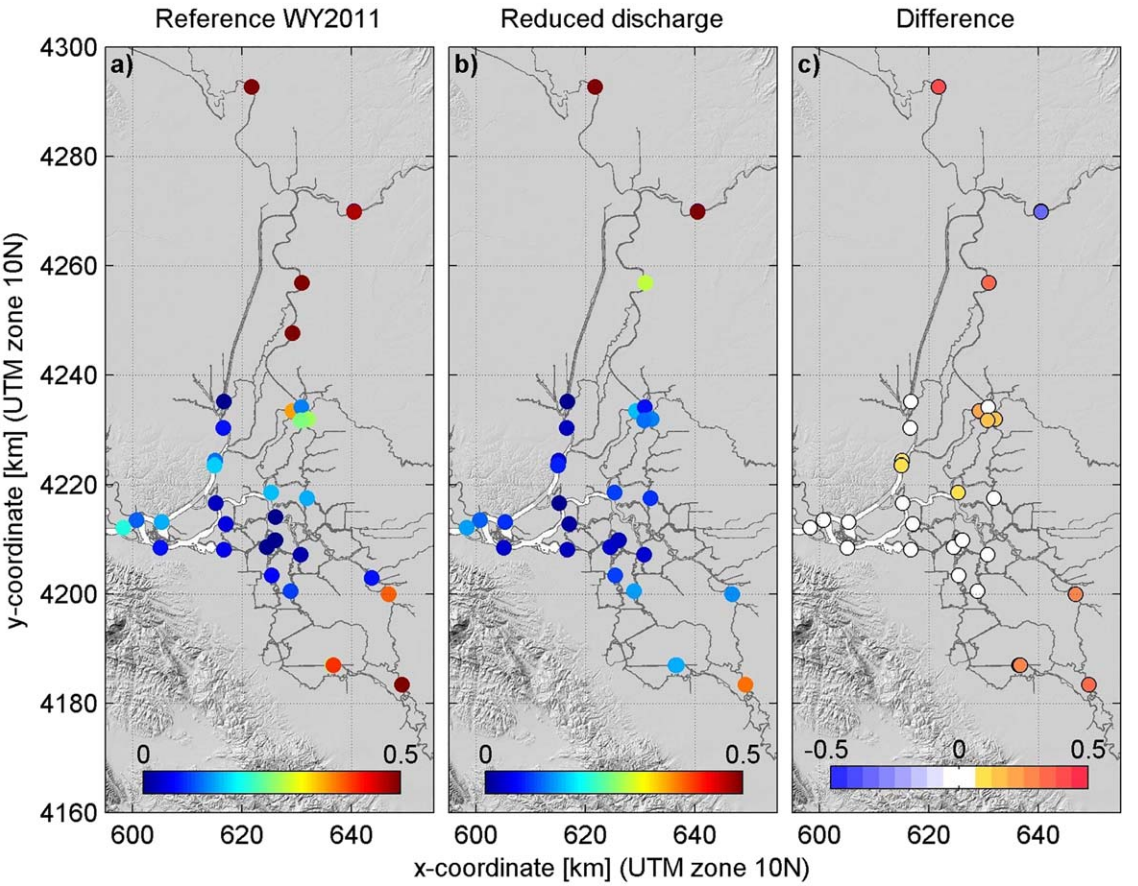

Figure 12. Residual velocity magnitude (m/s) for (a) reference WY2011, (b) reduced discharge, and (c) difference.

LPS. When the flow dynamics are altered as a result of reduced discharge, the heat exchange with the atmosphere becomes more important and relatively large differences in water temperature may occur. The potential increase in temperature during summer due to reduced discharges is in line with the observations of Jeffries et al. (2016) and Gleichauf (2015).

By changing the drivers of atmospheric forcing one-by-one, the influence of the different parameters was studied. For relative humidity and cloudiness, the minimum and maximum values (0% and 100%) were used to give the maximum variation. The variation of cloud cover is within the realistic range of clear-sky and cloudy conditions, and relative humidity is strongly variable over time and values range between 9% and 100% at Stockton in WY2011 (wunderground.com). Changing these highly variable values to a temporal and spatial constant set to an extremely high or extreme low value is not realistic, but gives insight into the relative importance of these parameters. Higher relative humidity will result in higher water temperature, as evaporation will diminish. Greater cloud cover will result in a lower water temperature, as more solar radiation will be blocked. This effect is larger than the reduction in effective back radiation, which will decrease with high cloud cover. The air temperature was increased and decreased by 5°C, based on Cayan et al. (2009), who provide an increase of 5°C in air temperature by 2100 as a maximum value for global warming scenarios. Figure 14 shows the modeled effect of variations in cloudiness, relative humidity, and air temperature on water temperatures in the Delta. The modeled effect of cloudiness is on average over the year less than 5°C; variations in relative humidity cause differences up to 10°C; and air temperature variations (from -5°C to $+5$°C) cause a water temperature difference exceeding 7°C, the latter depending on the air temperature variation applied (10°C in this case). The atmospheric forcing has for all three parameters the largest impact on the areas with lowest residual velocities (and presumably long residence times): the area around BAC and terminated sloughs with negligible flows, situated at the east side of the model domain.

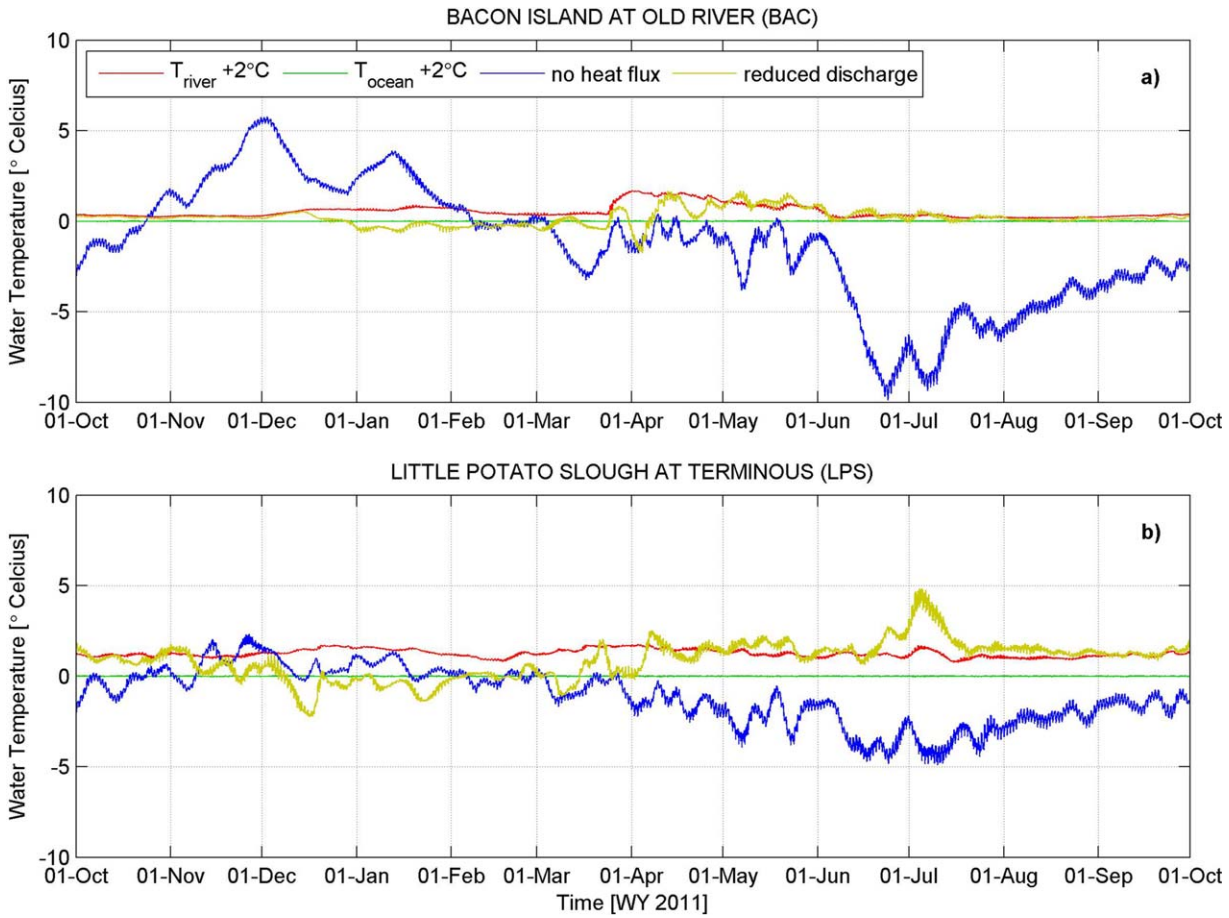

Figure 13. Water temperature at station (a) Bacon Island at Old River (BAC) and (b) Little Potato Slough at Terminous (LPS) for the simulation with increased river inflow temperature (red), the simulation with increased ocean temperature (green), the simulation without the heat flux model (blue), and the simulation with reduced discharge (yellowish line) relative to the reference simulation (2-D model for WY2011).

4. Discussion

The model is capable of reproducing observed temperature dynamics, including the seasonal, daily, and spatial variations, with a high degree of skill. The model did not require extensive calibration for the temperature dynamics, suggesting that both the hydrodynamic model and the heat exchange model cover dominant processes. The accuracy of the atmospheric forcing determines the model performance to a high degree, especially when residence times are long enough to allow for equilibrium between atmospheric forcing and water temperature. The model has a tendency to slightly under predict winter temperatures and to slightly over predict summer temperatures. These errors are more pronounced at some locations than others, possibly due to variations in residence time and water depth. A relatively small and short duration of the over prediction of the water temperatures in summer hampers the assessment of threshold values for certain species, such as Delta smelt (Brown et al., 2013, 2016; Wagner et al., 2011). Therefore, the present version of the model should be applied with caution when it is used to evaluate (changes in) such thresholds.

Stratification occurs in Central and North Bay, where salinity stratification strongly enhances the thermal stratification. When the entire model domain is converted to a 2-D model, the model performance is poor in this region, whereas the model performance in the Delta is not much affected. This implies that stratification in North Bay does not significantly affect water temperatures in the Delta under current conditions. An increase in ocean temperature will likely have an impact on 3-D processes in North Bay including slightly higher temperatures in general and slightly modified stratification. Still, temperature driven density currents should remain small compared to salinity-driven dynamics. Taking salinity intrusion as a proxy for ocean

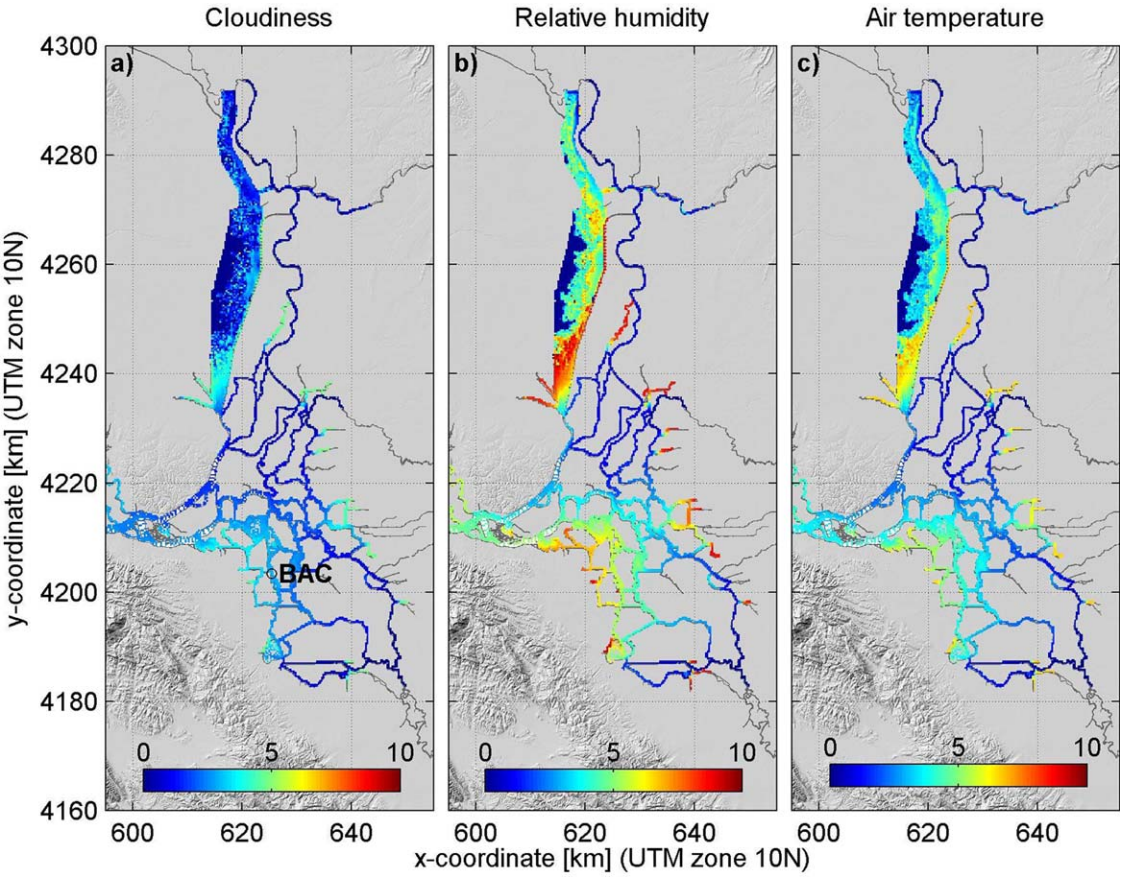

Figure 14. Yearly average water temperature difference per atmospheric forcing: (a) difference between 0% and 100% cloudiness, (b) difference between 100% and 0% relative humidity, and (c) difference between +5°C and −5°C in air temperature.

water moving landward, Delta temperatures will be hardly affected by intruding warmer ocean water, especially given the distance and, therefore, time for oceanic waters to equilibrate with the atmosphere before reaching the Delta. At some locations in the Delta thermal stratification may occur (temporarily), for example, in deep channels with relatively low flow velocities (e.g., near station RRI), or near closed gates and barriers (station GCT and DLC) where mixing of the water column is hampered due to limited hydrodynamic activity. The model reproduces but underestimates the thermal stratification, meaning that very weak temperature differences over the water column (<0.5°C) are not reproduced by the model, possibly due to too high vertical diffusivity in the model. However, the differences are of the same order of magnitude as the model error and are therefore too subtle to be reproduced. The model results suggest that although thermal stratification is occurring in the Delta, strong stratification is not widespread at the observation stations included in the model. The occurrence of thermal stratification at other locations than the observations stations could be part of further research.

Climate change might result in changing conditions at the model boundaries and changing atmospheric heat flux. Cayan et al. (2009) predict a loss of spring snowpack in California, which may alter the timing and amount of discharge from the upstream reservoirs. Gleichauf (2015) compared the "wet" year 2011 with the dry year of 2014 and found that water temperatures at the upstream boundary of tidal influence in the Sacramento River and the San Joaquin River differed significantly and that the drier 2014 had a higher inflow temperature compared to the wetter 2011, as a result of different residence times and atmospheric forcing. Cloern et al. (2011) state that decreasing snowmelt runoff does reduce the amount of cold water in upstream reservoirs, but that this does not affect the water temperature in the Delta significantly. Our study shows that reduced discharge could have a significant effect on water temperatures in certain parts of the Delta, which under "normal" conditions may be governed by upstream discharges but could become more impacted by atmospheric heat flux exchange as discharge decreases. The effect of changes in discharges is

dependent on the degree to which the water temperature is in equilibrium with the atmospheric heat flux, which may vary within the Delta. In the central Delta (around LPS), for example, the effect of the decrease in discharge is similar to an increase in water temperature of the upstream inflows with 2°C. The southwestern Delta (around BAC) is characterized by smaller residual velocities, potentially resulting in longer residence times and a larger impact of the atmospheric forcing. This implies that this region may be most prone to changes in atmospheric forcing, such as an increase in air temperature that is predicted in climate change scenarios (Cayan et al., 2009; Cloern et al., 2011). Spatial variations in the impact of upstream discharges and changing atmospheric forcing imply that water management (i.e., reservoir operations, operations of weirs, and barriers) to affect water temperatures may be more effective for some locations than for others. It should be noted that management of water temperature for multiple species in this estuarine ecosystem is complicated and worthy of future (e.g., model based) study.

Changing relative humidity by 100% and air temperature by 10°C results in similar ranges in computed water temperatures, while the impact of cloudiness (100% range) is smaller. The increase in air temperature applied to the model is in agreement with predictions by Cayan et al. (2009), who project an air temperature increase of 1–3°C in 2050 and an increase of 2–5°C by 2100 based on two greenhouse gas emission scenarios and six Global Climate Models (GCMs). The ranges applied for relative humidity and cloudiness in this study are absolute maxima and minima, uniform in space and time, and far from realistic. When the relative humidity is 100%, less evaporation can take place and the water temperature rises drastically (and vice versa for low relative humidity). The relative humidity is dependent on the absolute humidity and the air temperature. Relative humidity for climate change scenarios need to incorporate this dependency.

Sensitivity tests were executed to study the impact of changes in forcing parameters separately, whereas in reality the atmospheric and boundary forcings are coupled. An increase in air temperature might affect the relative humidity and cloudiness, as well as the ocean and river inflow temperatures. These linkages between forcings have been neglected herein in order to be able to distinguish the influence of different forcing parameters from each other. The next application of this model as part of a series of linked hydrodynamic, temperature and ecosystem models within the CASCaDE project will be the assessment of climate and infrastructure change scenarios. Climate change scenarios will include changes in multiple mutually consistent forcing parameters, which may interact with each other. Model improvement can be achieved by using better atmospheric forcing values including wind forcing, as the model performance is better during high discharges in spring, when the flow rates are higher and the relative impact of the atmospheric forcing is lower. For example the air temperature over the day is schematized from daily minimum and maximum values, which is not as accurate as hourly observed values. Station Dutch Slough at Jersey Island (DSJ), situated within the southwestern Delta where the atmospheric forcing has a large impact, shows a weaker agreement with observations than other stations (see supporting information), indicating that improving the atmospheric forcing might result in even better model performance. Other processes that may enhance model performance are exchanges with the bed and ground water. Exchange with the ground water (not currently included in the model) might increase winter temperatures and decrease summer temperatures, as the ground water temperature has less variation over the year. Bed heat exchange is currently being implemented, and preliminary results show an improvement of temperature predictions in shallow areas (<Secchi depth), but little effect in the deeper areas. The current state of the model assumes that radiation heats shallow water, while the bed absorbs the remaining radiation. New versions will consider (back) radiation from the bed, slightly increasing mean water temperatures but also dampening temperature variations in shallow water. Finally, further improvement of the hydrodynamic model may take place by including freshwater supply in South Bay and including gate operations at the Clifton Court forebay in the southern Delta (near Tracy pumping plant) and Sand Mound Slough in the southwestern Delta (near Rock Slough pumping plant) (Martyr-Koller et al., 2017).

5. Conclusions

The Delft3D-Flexible Mesh Model reproduces the observed temperature dynamics in the San Francisco Bay-Delta system with significant skill. The seasonal variation over the year is well reproduced, as are the daily temperature variations at many locations. This model behavior is obtained without extensive calibration of the temperature model itself, but used a calibrated and validated hydrodynamic model including salinity

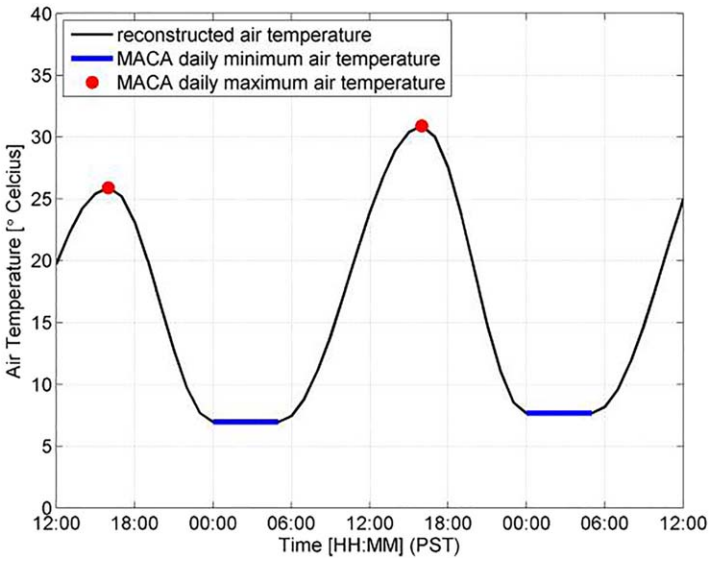

Figure A1. Reconstructing an hourly air temperature signal from daily minimum and maximum Livneh air temperatures.

dynamics as a basis. The model was able to reproduce observed water temperatures well for water year 2012, which was dry ("below normal") and hence had low discharge rates.

North Bay shows thermal stratification, strongly enhanced by 3-D salinity dynamics. The model is able to reproduce this stratification, although weak stratification, with temperature differences on the order of the model error, is not reproduced. As complex 3-D dynamics appear largely absent in the Delta, a 2-D model was used to study the effect of different drivers on the temperature dynamics in this area, saving computational time. The 2-D model showed significant skill for the water temperature in the Delta at most stations.

The impact of changing forcings varies throughout the Delta. We hypothesize that this spatial variation in sensitivity is, at least in part, a result of variations in flow rates and, consequently, the impacts of the heat flux exchange with the atmosphere. When the residual velocity is small and the residence time is likely longer, there is more time for exchange of heat with the atmosphere and the local water temperature can reach an equilibrium with the atmospheric forcing at that location. An increase in ocean temperature does not affect the modeled temperature dynamics in the Delta, given other forcing parameters do not

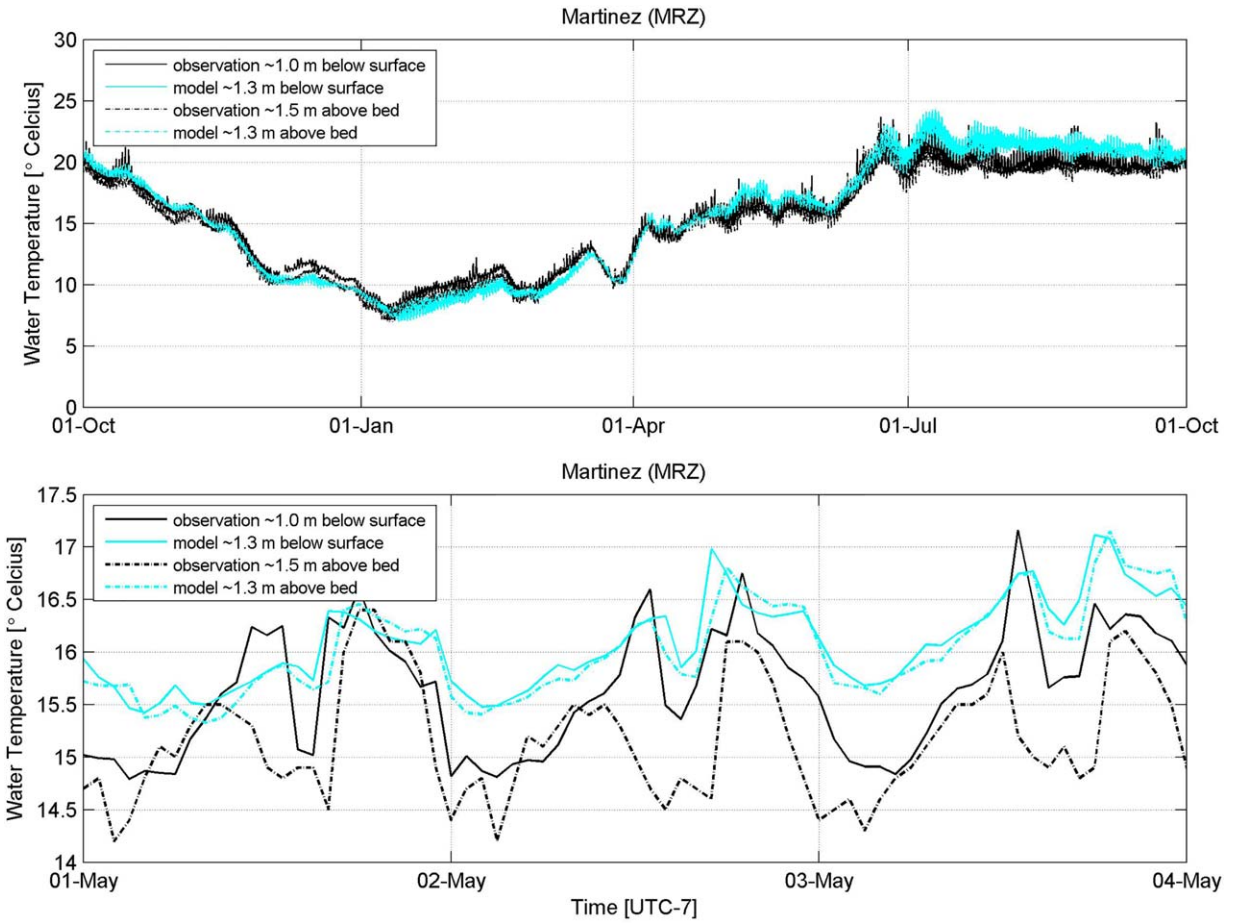

Figure A2. Observed water temperature at the surface (black) and near the bed (blue) and computed water temperature at the surface (orange) and near the bed (cyan) at station Martinez (MRZ) for water year 2011 (top) and zoomed to 3 days in May (bottom).

change. The impact of increasing inflow temperature at the model's upstream boundaries decreases with increasing distance from inflow points. For the ranges of forcings explored in this study, the southwestern Delta is most sensitive to changes in the atmospheric forcing (relative humidity, air temperature, and cloudiness), but less sensitive to changes in inflow temperatures and magnitudes of upstream discharges.

Appendix A

Figure A1 shows how a daily varying air temperature was reconstructed from minimum and maximum Livneh air temperatures.

The following formula was used to convert the specific humidity to relative humidity:

$$R_{hum} = \frac{0.263 * P_{atm} * S_{hum}}{e^{\left(\frac{17.67 * T_{air}}{T_{air}+243.5}\right)}}$$

with R_{hum} is the relative humidity (%); P_{atm} is the atmospheric pressure (Pa); S_{hum} is the specific humidity (–); and T_{air} is the air temperature (°C).

The following formula was used to convert the downward solar radiation to cloudiness:

$$Cloudiness = \frac{0.4 - \left(0.16 + 1.52 * \left[1 - \frac{Q_{dw}}{Q_{cs}}\right]^{0.5}\right)}{-0.76} * 100$$

with Cloudiness is the percentage of clear-sky solar radiation blocked by clouds (%); Q_{dw} is the downward solar radiation at ground level (W/m^2); and Q_{cs} is the clear-sky solar radiation at ground level (W/m^2).

Figure A2 shows observed thermal stratification at Martinez Station and too small temperature variations in the model.

Acknowledgments
The research is carried out within the framework of the U.S. Geological Survey Computational Assessment of Scenarios of Change for the Delta Ecosystem (CASCaDE). Funding support was provided by the Delta Stewardship Council/Delta Science Program, USGS Priority Ecosystems Science/Priority Landscapes, USGS Hydrologic Research and Development/Water Availability and Use/National Water Quality Program, and the San Francisco Bay Nutrient Management Strategy and the San Francisco Bay Regional Monitoring Program (via the San Francisco Estuary Institute). The authors acknowledge the San Francisco Estuary Institute for making this research financially possible. We thank Mike Dempsey, Rolf Frankenbach, Matthew Mulligan, Jay Aldrich, and Kenneth Karcher from the California Department of Water Resources, for making the observation data and/or metadata freely available. Water temperatures observations were also collected from CDEC (http://cdec.water.ca.gov/), CENCOOS (data.cencoos.org), and USGS (waterdata.usgs.gov/) websites. We thank Doug Sinton of San Jose State University for the wind data and Noah Knowles from the U.S. Geological Survey for facilitating our use of the ROMS water temperature boundary data as well as the METDATA and Livneh atmospheric forcings, and for his helpful comments and modeling support. We thank Herman Kernkamp and Arthur van Dam from Deltares for their work on software improvement and modeling support. We thank Larry Brown and two anonymous reviewers for their insightful suggestions. The model and its input conditions are being made publicly available at www.d3d-baydelta.org and http://californiacoastalatlas.net/. This is CASCaDE 2 contribution 74.

References

Abatzoglou, J. T. (2011). Development of gridded surface meteorological data for ecological applications and modelling. *International Journal of Climatology*, *33*, 121–131. https://doi.org/10.1002/joc.3413

Achete, F. M., van der Wegen, M., Roelvink, D., & Jaffe, B. (2015). A 2-D process-based model for suspended sediment dynamics: A first step towards ecological modeling. *Hydrology and Earth System Sciences*, *19*, 2837–2857. https://doi.org/10.5194/hess-19-2837-2015

Andrew, J. T., & Sauquet, E. (2017). Climate change impacts and water management adaptation in two Mediterranean-climate watersheds: Learning from the Durance and Sacramento Rivers. *Water*, *9*(2), 126. https://doi.org/10.3390/w9020126

Bartholow, J. M. (1989). *Stream temperature investigations: Field and analytic methods*. (Instream Flow Inf. Pap. 13, Biol. Rep. 89(17), 139 p.). Washington, DC: U.S. Fish and Wildlife Service.

Brown, L. R., Bennett, W. A., Wagner, R. W., Morgan-King, T., Knowles, N., Feyrer, F.,. . . Dettinger, M. (2013). Implications for future survival of Delta smelt from four climate change scenarios for the Sacramento-San Joaquin Delta, California. *Estuaries and Coasts*, *36*(4), 754–774. https://doi.org/10.1007/s12237-013-9585-4

Brown, L. R., Komoroske, L. M., Wagner, R. W., Morgan-King, T., May, J. T., Connon, R. E., & Fangue, N. A. (2016). Coupled downscaled climate models and ecophysiological metrics forecast habitat compression for an endangered estuarine fish. *PLoS One*, *11*(1), e0146724. https://doi.org/10.1371/journal.pone.0146724

Cayan, D., Tyree, M., Dettinger, M., Hidalgo, H., Das, T., Maurer, E.,. . . Flick, R. (2009). *Climate change scenarios and sea level rise estimates for the California 2009 climate change scenarios assessment* (California Energy Comm. Rep. CEC-500–2009-014-F). Sacramento, CA: California Climate Change Center.

Cloern, J. E., Knowles, N., Brown, L. R., Cayan, D., Dettinger, M. D., Morgan, T. L.,. . . & Jassby, A. D. (2011). Projected evolution of California's San Francisco Bay-Delta-River System in a century of climate change. *PLoS One*, *6*(9), e24465. https://doi.org/10.1371/journal.pone.0024465

Cloern, J. E., & Schraga, T. S. (2016). *USGS measurements of water quality in San Francisco Bay (CA), 1969–2015: U. S. Geological Survey data release*. San Francisco Bay-Delta: National Research Program. https://doi.org/10.5066/F7TQ5ZPR

Fregoso, T. A., Wang, R.-F., Alteljevich, E., & Jaffe, B. E. (2017). *San Francisco Bay-Delta bathymetric/topographic digital elevation model (DEM): U.S. Geological Survey data release.* San Francisco Bay-Delta: Pacific Coastal and Marine Science Center. https://doi.org/10.5066/F7GH9G27

Gleichauf, K. T. (2015). *Temperature and tidal river junction dynamics in the Sacramento-San Joaquin Delta, California* (Dissertation). Stanford, CA: Stanford University. Retrieved from http://purl.stanford.edu/dq848xb0777

Grimaldo, L. F., Sommer, T., Van Ark, N., Jones, G., Holland, E., Moyle, P.,. . . Smith, P. (2009). Factors affecting fish entrainment into massive water diversions in a tidal freshwater estuary: Can fish losses be managed? *North American Journal of Fisheries Management*, *29*, 1253–1270.

Jassby, A. D., Kimmerer, W. J., Monismith, S. G., Armor, C., Cloern, J. E., Powell, T. M.,. . . Vendlinski, T. J. (1995). Isohaline position as a habitat indicator for estuarine populations. *Ecological Applications*, *5*, 272–289. https://doi.org/10.2307/1942069

Jeffries, K. M., Connon, R. E., Davis, B. E., Komoroske, L. M., Britton, M. T., Sommer, T., . . . Fangue, N. A. (2016). Effects of high temperatures on threatened estuarine fishes during periods of extreme drought. *Journal of Experimental Biology*, *219*, 1705–1706. https://doi.org/10.1242/jeb.134528

Jolliff, J., Kindle, J., Shulman, I., Penta, B., Friedrichs, M., Helber, R., & Arnone, R. (2009). Summary diagrams for coupled hydrodynamic-ecosystem model skill assessment. *Journal of Marine Systems*, *76*, 46–82.

Kimmerer, W. (2002). Physical, biological, and management responses to variable freshwater flow into the San Francisco Estuary. *Estuaries*, *25*(6), 1275–1290.

Livneh, B., Bohn, T. J., Pierce, D. W., Munoz-Arriola, F., Nijssen, B., Vose, R.,. . . & Brekke, L. (2015). *A spatially comprehensive, meteorological data set for Mexico, the U.S., and southern Canada (NCEI Accession 0129374). Version 1.1*. NOAA National Centers for Environmental Information. Retrieved from https://doi.org/10.7289/V5X34VF6; https://doi.org/10.1038/sdata.2015.42

Ludwig, F. L., & Sinton, D. (2000). Evaluating an objective wind analysis technique with a long 25 record of routinely collected data. *Journal of Applied Meteorology*, *39*, 335–348.

Martyr-Koller, R. C., Kernkamp, H., van Dam, A., van der Wegen, M., Lucas, L. V., Knowles, N.,. . . & Fregoso, T. (2017). Application of an unstructured 3D finite volume numerical model to flows and salinity dynamics in the San Francisco Bay-Delta. *Estuarine, Coastal and Shelf Science*, *192*, 86–107. https://doi.org/10.1016/j.ecss.2017.04.024

Miller, R. L., & Kamykowski, D. L. (1986). Effects of temperature, salinity, irradiance and diurnal periodicity on growth and photosynthesis in the diatom Nitzschia Americana: Light-saturated growth. *Journal of Phycology*, *22*, 339–348. https://doi.org/10.1111/j.1529-8817.1986.tb00033.x

Monismith, S. G., Genin, A., Reidenbach, M., Yahel, G., & Koseff, J. R. (2006). Thermally driven exchanges between a coral reef and the adjoining ocean. *Journal of Physical Oceanography*, *36*, 1332–1347.

Monismith, S. G., Hench, J. L., Fong, D. A., Nidzieko, N. J., Fleenor, W. E., Doyle, L. P., & Schladow, S. G. (2009). Thermal variability in a tidal river. *Estuaries and Coasts*, *32*, 100–110. https://doi.org/10.1007/s12237-008-9109-9

Monismith, S. G., Imberger, J., & Morison, M. L. (1990). Convective motions in the sidearm of a small reservoir. *Limnology & Oceanography*, *35*(8), 1676–1702.

Monsen, N. E., Cloern, J. E., Lucas, L. V., & Monismith, S. G. (2002). A comment on the use of flushing time, residence time and age as transport time scales. *Limnology and Oceanography*, *47*(5), 1545–1553.

Neveu, E., Moore, A. M., Edwards, C. A., Fiechter, J., Drake, P., Crawford, W. J., . . . Nuss, E. (2016). An historical analysis of the California current circulation using ROMS 4D-Var: System configuration and diagnostics. *Ocean Modelling*, *99*, 133–151. https://doi.org/10.1016/j.ocemod.2015.11.012

Ralston, D. K., Brosnahan, M. L., Fox, S. E., Lee, K., & Anderson, D. M. (2015). Temperature and residence time controls on an estuarine harmful algal bloom: Modeling hydrodynamics and *Alexandrium fundyense* in Nauset estuary. *Estuaries and Coasts*, *38*(6), 2240–2258.

Schraga, T. S., & Cloern, J. E. (2017). Water quality measurement in San Francisco Bay by the U.S. Geological Survey, 1969–2015. *Scientific Data*, *4*, 170098. https://doi.org/10.1038/sdata.2017.98

Sturman, J. J., Oldham, C. E., & Ivey, G. N. (1999). Steady convective exchange flows down slopes. *Aquatic Sciences*, *61*, 260–278. (1999)

Swanson, C., Reid, T., Young, P. S., & Cech, J. J. Jr. (2000). Comparative environmental tolerances of threatened delta smelt (*Hypomesus transpacificus*) and introduce wakasagi (*H. nipponensis*) in an altered California estuary. *Oecologia*, *123*, 384–390.

Underwood, G. J. C., & Kromkamp, J. (1999). Primary production by phytoplankton and microphytobenthos in estuaries. *Advances in Ecological Research*, *29*, 93–153.

Wagner, R. W., Stacey, M., Brown, L. R., & Dettinger, M. (2011). Statistical models of temperature in the Sacramento-San Joaquin Delta under climate-change scenarios and ecological implications. *Estuaries and Coasts*, *34*, 544–566. https://doi.org/10.1007/s12237-010-9369-z